Low symmetry configurations of vacancy-oxygen complexes in irradiated silicon

Y. Kusano,[1] H. Saito,[1] L. S. Vlasenko,[2] M. P. Vlasenko,[2] E. Ohta,[1] and K. M. Itoh[1,a)]
[1]*School of Fundamental Science and Technology, Keio University, 3-14-1 Hiyoshi, Kohoku-ku, Yokohama 223-8522, Japan*
[2]*A.F. Ioffe Physico-Technical Institute, Russian Academy of Sciences, St. Petersburg 194021, Russia*

(Received 8 November 2015; accepted 8 December 2015; published online 28 December 2015)

Two new electron paramagnetic resonance (EPR) spectra, labeled KU2 and KU3, emerge as a result of annealing of γ-ray irradiated silicon crystals in the temperature range 360–560 °C. The EPR intensities of KU2 and KU3 increase in the upper range of the annealing temperature where the EPR peaks of the vacancy-oxygen complex (A-center) diminish. The angular dependence study shows that the EPR spectra of KU2 and KU3 resemble that of SL1, the excited triplet (spin $S = 1$) state of A-centers, but with slightly different $\boldsymbol{g}$ and $\boldsymbol{D}$-tensors representing lowering in symmetries. Microscopic lattice distortions caused by capturing of extra interstitial oxygen atoms by the A-centers are proposed to be the source of lowering of the symmetries associated with KU2 and KU3. © *2015 AIP Publishing LLC*. [http://dx.doi.org/10.1063/1.4938199]

I. INTRODUCTION

Irradiation of semiconductors by high-energy particles produces various defects. While irradiation technologies such as ion implantation play very important roles in the silicon integrated circuit (Si IC) fabrication, irradiations on fully processed Si IC are often known to degrade their device performances.[1] Radiation induced defects in silicon have been investigated intensively over the past 50 years using a variety of characterization methods, including electron paramagnetic resonance (EPR) spectroscopy,[2,3] to reveal the microscopic structures of paramagnetic defects.

When Czochralski grown silicon (Cz-Si), i.e., the crystal containing the concentration of oxygen at the level of 1×10^{18} cm^{-3}, is exposed to electron or γ-ray irradiations at room temperature, vacancy-oxygen pairs (VO), referred to as A-centers, are produced predominantly. A singly negative charge state of the A-center leads to the spin $S = 1/2$ EPR spectrum known as B1.[4,5] It has been also shown that the band-gap light illumination transforms A-centers to spin triplet ($S = 1$) centers referred to as SL1 centers.[6] This SL1 center has been studied by both continuous wave and pulsed EPR methods.[7] Heat-treatments of Cz-Si before and/or after the irradiations make oxygen atoms mobile leading to formation of oxygen aggregates.[8–10] For example, infrared (IR) spectroscopy studies have revealed formation of VO_2 and VO_3 complexes.[8,10] New energy levels were found using deep level transient spectroscopy (DLTS) in oxygen-rich silicon subjected to heat treatment before irradiation.[11,12] Considering the motion of vacancies and oxygen atoms released under annealing of irradiated Cz-Si, EPR spectroscopy studies have identified formation of V_2, VO, and V_2O complexes after annealing below 350 °C, and of V_2O_2, V_3O, V_3O_2, and V_3O_3 complexes after annealing at higher temperatures.[9]

The present study reports EPR investigation under the band-gap light illumination of vacancy-oxygen complexes in γ-irradiated Cz-Si crystals. Systematic isochronal annealing investigations in the temperature range of 200–560 °C lead to observation of two new spin $S = 1$ EPR spectra we label KU2 and KU3. Angular dependences of KU2 and KU3 EPR line positions allow us to determine the spin Hamiltonian parameters and symmetry of each complex. We suggest that KU2 and KU3 arise from the excited triplet state of A-centers, i.e., similar to the case of SL1, but their symmetries are lowered by capture of extra oxygen atoms nearby to form more complex structures.

II. EXPERIMENT

Two types of samples were prepared from Czochralski grown *n*-type phosphorus doped silicon with the resistivity $\rho \sim 100\,\Omega$cm and $2\,\Omega$cm, respectively. The size of the samples was $10 \times 3 \times 1$ mm^3 with the long edge oriented along ⟨110⟩ axis. The samples were irradiated by γ-rays with the dose of $\sim 10^{19}$ cm^{-2} using a ^{60}Co source at room temperature.

The EPR measurements were performed with an X-band (9 GHz) EPR spectrometer (JEOL JES-RE3X) with a cylindrical TE_{011}-mode cavity and 100 kHz magnetic field modulation. The second derivatives of the absorption signals were detected to get better resolution of EPR spectra. During the measurements, the temperature of the samples was kept at 25 K using an Oxford Instruments ESR900 helium-gas-flow cryostat and illumination by white light was kept continuously through an optical window using a 100 W halogen lamp.

Annealings of the samples were performed in argon atmosphere for 10 min from the temperature of 200 °C to 560 °C with the step of 20 °C. After each annealing, EPR spectrum was recorded using the condition stated earlier. The angular dependences of the EPR spectra were determined by rotating the sample around ⟨110⟩ axis.

a)Author to whom correspondence should be addressed. Electronic mail: kitoh@appi.keio.ac.jp

III. RESULTS AND DISCUSSION

The most visible paramagnetic defect created by the γ-irradiation of Cz-Si is the vacancy-oxygen complex (A-center). Therefore, as shown in Fig. 1, the irradiated samples show strong EPR spectrum of SL1[6] when measured with the band-gap illumination, since the most of A-centers are optically excited to the metastable spin $S=1$ state giving SL1 spectrum. However, after a certain annealing condition as shown in Fig. 1(b), EPR with illumination leads to emergence of new spectra of excited spin $S=1$ states which we label KU2 and KU3. The naming here follows the numbering sequence of the previously discovered KU1 defect in silicon, also $S=1$, at Keio University (KU).[13] Compared with SL1, KU2 and KU3 show larger fine structure splittings and additional splitting of some lines, indicating the lowering of the symmetry. Note that only SL1 centers are observed before and after annealing below 300 °C.

Figure 2 shows the annealing temperature dependences of the EPR line intensity for the orientation B || ⟨110⟩. It can be seen that the systematic isochronal annealing of the irradiated samples for 10 min above 300 °C leads to the gradual decrease in the intensity of SL1 spectra and emergence of KU2 and KU3 for the temperature window between 380 °C and 550 °C.

Fine structure of spin $S=1$ spectra is described by Hamiltonian

$$\boldsymbol{H} = g\beta\boldsymbol{BS} + \boldsymbol{SDS}, \tag{1}$$

where β is the Bohr magnetron, $\boldsymbol{g}$ is the tensor, and $\boldsymbol{D}$ is the traceless tensor describing the dipole–dipole interaction between a pair of electrons forming spin $S=1$. The contribution of spin–orbit interaction to the second term in Eq. (1) is negligible for the centers considered in the present paper.[6] In order to convincingly show that we have indeed identified new defects, it is important to build up our logic starting from A-center. The coordinate system and positions of Si atoms for A-center in undistorted silicon lattice is shown in

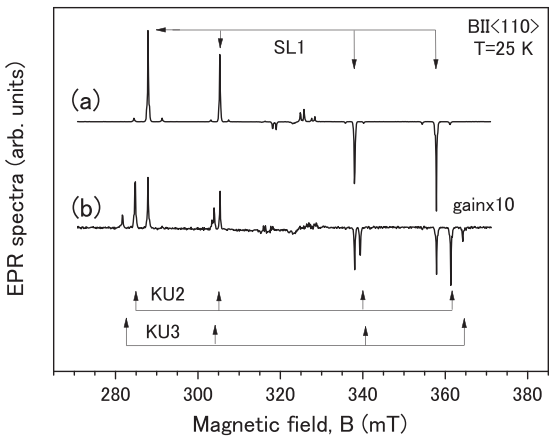

FIG. 1. EPR spectra observed in γ-irradiated Cz-Si (2 Ω cm): (a) after irradiation and (b) after annealing at 400 °C. Weak satellite lines near each Zeeman line of SL1 spectrum visible in (a) originate from the hyperfine interaction with ^{29}Si nuclei occupying two equivalent places. The EPR spectra were measured at 25 K with B||⟨110⟩ and continuous illumination of band gap light.

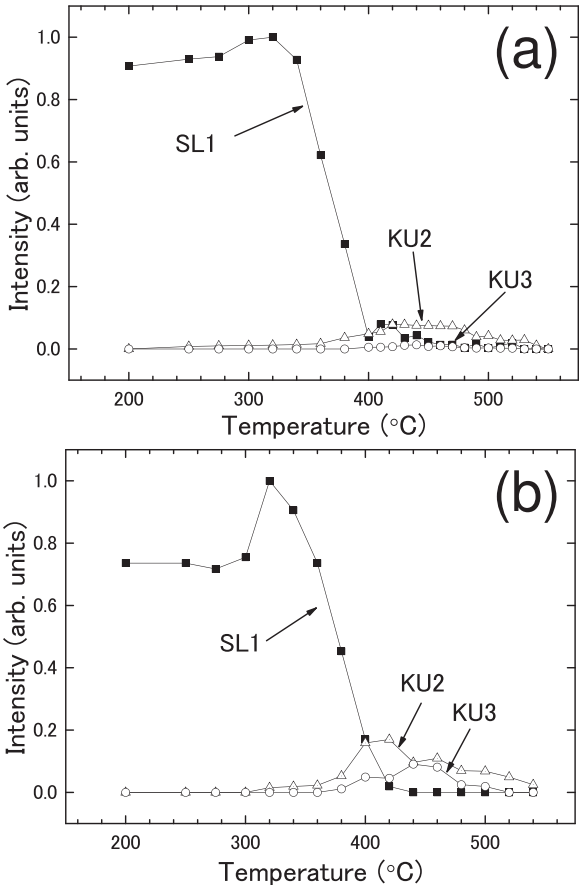

FIG. 2. Dependences of the relative intensities of SL1, KU2, and KU3 EPR spectra on the annealing temperature for (a) 2 Ω cm and (b) 100 Ω cm samples. The EPR spectra were measured at 25 K with B||⟨110⟩ and continuous illumination of band gap light.

Fig. 3. Single oxygen atom represented by an open circle residing near the vacancy site near the center of cube forms two bonds with any two silicon atoms at a, b, c, and d. The remaining two Si dangling bonds form the bonding and antibonding molecular orbitals containing two electrons with

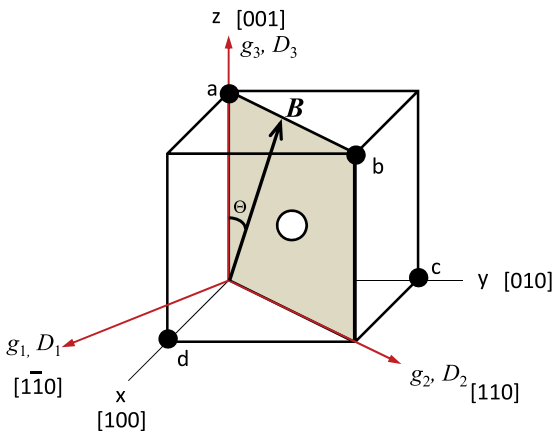

FIG. 3. Cartesian coordinates (x, y, z), positions of Si atoms (filled circles a, b, c, d), and the principal symmetry axes (1, 2, 3) for single A-center. The angular dependence of the EPR spectra was measured from [001] to [110] with the magnetic field $\boldsymbol{B}$ applied within the shaded [1$\bar{1}$0] plane. Θ is the angle between magnetic field $\boldsymbol{B}$ and [001] crystal axis. An oxygen atom (open circle) captured at the vacancy site near the center of the cube forms two bonds with silicon atoms located at a, b, c, and d.

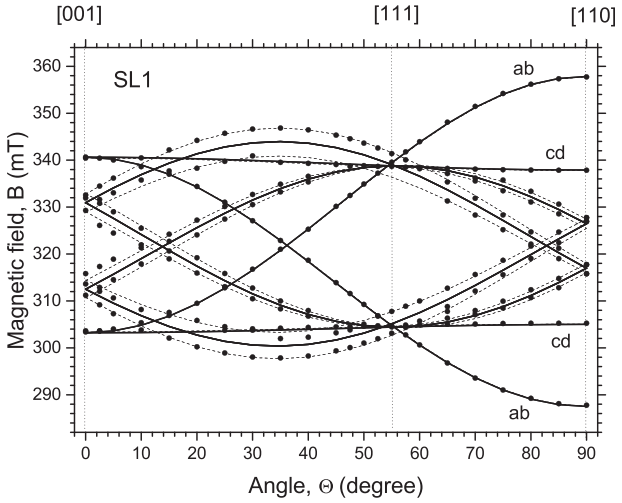

FIG. 4. Filled circles show experimentally obtained angular dependence of the line positions for SL1 peaks in the present studies. Solid lines are calculated dependence using the previously determined parameters as listed in Table I. Dashed lines show calculations taking into account the misorientation of sample by 3° within the (110) plane in Fig. 3 leading to splitting of some lines. The lines labeled *ab* and *cd* represent the cases when the oxygen atom is forming bonds with a-b and c-d, respectively, in Fig. 3. Microwave frequency is $f = 9.0580$ GHz.

parallel spins. The defect has six equivalent ⟨110⟩ axes connecting a-b, a-c, a-d, b-c, b-d, and c-d. This well-established model of A-center and EPR investigations of B1 without illumination[4,5] and SL1 with illumination[6] show that both B1 and SL1 spectra have the orthorhombic (C_{2v}) symmetry. Fig. 4 shows the experimental positions of SL1 EPR lines measured with the samples employed in this study. Employing the Hamiltonian parameters for SL1 determined in Ref. 6, which are listed in Table I, the angular dependence of SL1 line positions agrees very well with the calculation. When the magnetic field $\boldsymbol{B}$ is precisely in $(1\bar{1}0)$ rotation plane, the number of EPR lines should equal to 8. Even a few degrees of misorientation of the sample leads to further splitting of the lines; however, the total number should not exceed 12 for the orthorhombic symmetry. The experimental points in Fig. 4 show such splittings for lines when the oxygen atom is forming bonds with a-c, a-d, b-c, and b-d (see Fig. 3). It should be noted that the lines corresponding to a-b and c-d orientations do not split under any misorientations of the magnetic field for SL1. Having confirmed the reproducibility of SL1 spectra in our samples, we shall now move onto analysis of KU2 and KU3. Figure 5 shows further splittings of KU2 in the c-d direction and KU3 in the a-b direction. Such splitting of *ab* and *cd* lines clearly shows that the symmetries of these defects are lowered from the orthorhombic of SL1. Furthermore, the number of lines for KU2 spectrum exceeds 12. Angular dependences of these spectra are well described by Eq. (1) with $\boldsymbol{g}$ and $\boldsymbol{D}$ tensors having the monoclinic (C_{1h}) symmetry. Principal values of these tensors determined by analyzing the angular dependences of KU2 and KU3 are shown in Table I. The experimental and calculated angular dependences for KU2 and KU3 EPR spectra are shown in Fig. 6.

Hamiltonian parameters of KU2 and KU3 spectra listed in the Table I are similar to those of SL1 spectrum. In addition, the hyperfine satellites are observed for $B \,||\, \langle 110 \rangle$ and the line shapes of these spectra shown in Fig. 7 are similar. The intensities of the hyperfine structure lines with splitting of 6.7 mT and 7.4 mT for SL1 and KU2, respectively, correspond to the hyperfine interaction with ^{29}Si nucleus existing with the natural abundance of 4.7% and they can occupy the two nearest sites to the A-center. Three times stronger lines near the wings of central lines are caused by the hyperfine interaction with ^{29}Si nuclei located at the next six nearest sites of the silicon lattice to the A-center. Similarity in the spectra and emergence-disappearance correlation between SL1, KU2, and KU3 (Fig. 2) leads us to suggest that the EPR spectra KU2 and KU3 arise from the excited triplet states of the distorted A-centers. For example, the lattice distortion near the A-center can be produced by capturing of interstitial oxygen atoms that are made mobile at high temperatures.

A suggested model of the KU2 and KU3 involving capturing of one oxygen atom near the A-center is shown in Fig. 8. Oxygen atom can be captured between the bond b-g and shifts the Si atom at b in $(1\bar{1}0)$- plane toward the extension of the bond b-g as shown in Fig. 8 by a open red circle.

TABLE I. Hamiltonian (Eq. (1)) parameters of the observed spin $S = 1$ EPR spectra. Principal values of g_i and D_i $(i = 1,2,3)$ for SL1 spectrum are given with respect to exact axes shown in Fig. 3. For KU2 and KU3 spectra the principal axes were obtained from (1,2,3) axes by additional rotation around the axis 2 for ±12° for KU2, and around the axis 1 for ±2° for KU3 spectrum. Alternatively, the principal axes can be found by rotation around (X,Y,Z) axes using the Euler angels $(\alpha\beta\gamma)$: (45°, 0°, 0°) for SL1, (−45°, ±0°, 90°) for KU2, and (45°, ±2°, 0°) for KU3. Errors are ±0.0002 for the $\boldsymbol{g}$-components and ±1 MHz for the $\boldsymbol{D}$-components.

Spectrum	g_1	g_2	g_3	D_1 (MHz)	D_2 (MHz)	D_3 (MHz)
SL1[a]	2.0102	2.0057	2.0075	±308	∓658	±350
KU2	2.0080	2.0040	2.0070	±332	∓718	±386
KU3	2.0085	2.0035	2.0060	±340	∓775	±435

[a]Values are taken from Ref. 6.

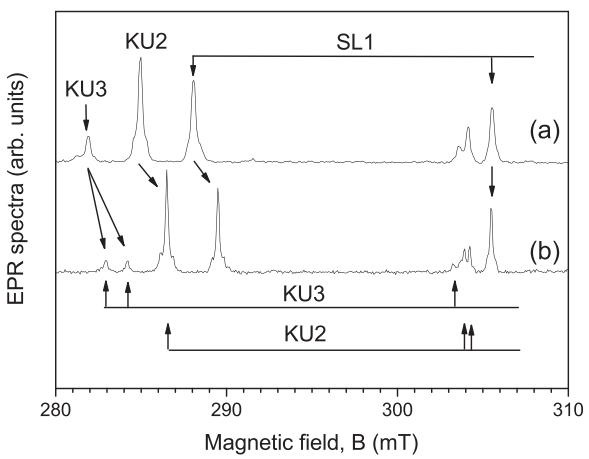

FIG. 5. Splittings of EPR lines of KU2 and KU3 spectra under rotation of the sample. The 100 Ωcm sample after annealing at 420 °C measured with (a) $B \,||\, \langle 110 \rangle$ so that $\Theta = 0°$ and (b) $\Theta = 10°$ between B and ⟨110⟩ axis. The left side of lines, 280–290 mT, corresponds to the a-b orientation, while the right side, 304–308 mT, to the c-d orientation as defined in Fig. 3.

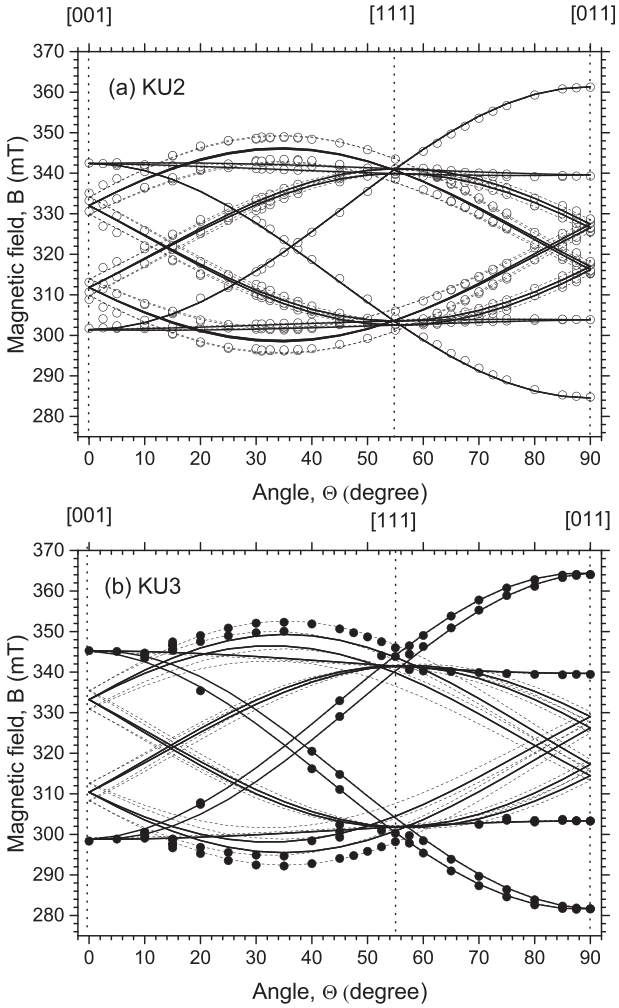

FIG. 6. Angular dependence of the line positions of (a) KU2 and (b) KU3 spectra. Circles are experimental results and solid lines are calculations with Eq. (1) using the parameters listed in Table I. Dashed lines are calculations with experimentally unavoidable misorientation of the sample by 3° within the (110) plane as was done in Fig. 4. Experimental positions of KU3 peaks are not fully resolved between 300 and 340 mT since the intensities of KU3 are much weaker than those of KU2 that are masking the KU3 peaks.

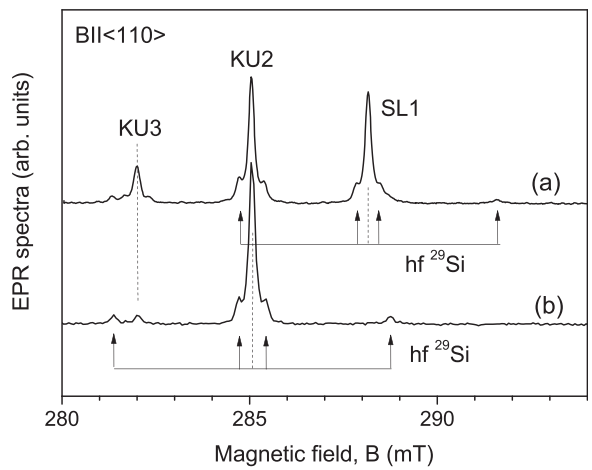

FIG. 7. Low field lines of EPR spectra observed in the 100 Ω cm sample annealed at (a) 420 °C and (b) 460 °C. The arrows show hyperfine structure due to the nearest ^{29}Si nuclei.

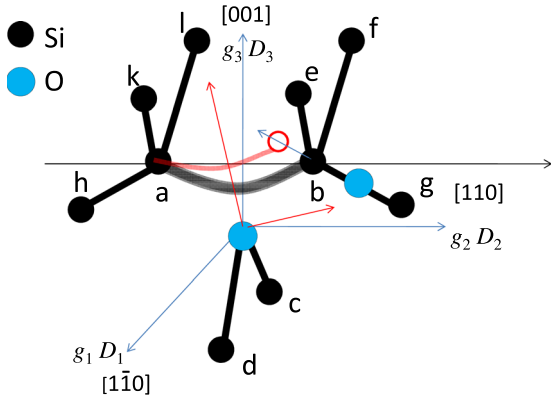

FIG. 8. A microscopic structure model of the A-center with additional one oxygen atom (blue) captured at the nearest Si-Si bond. The red circle is a Si atom displaced from the position b as the result of insertion of an oxygen atom between the Si bond b-g.

This rotates the principal axes 2 and 3 to the position shown by red arrows to change or lower the symmetry from the orthorhombic (C_{2v}) to monoclinic (C_{1h}). Similarly, capturing of an oxygen atom between the equivalent a-h bond leads to rotation of the 2 and 3 axes in the opposite direction. This model can produce the observed angular dependence of KU3 spectrum shown in Fig. 6(b). Additional possibilities for the location of the extra oxygen atom are between the equivalent bonds b-e, b-f, a-k, and a-l (see Fig. 8). We suggest that such configurations of defect are responsible for KU2 EPR spectrum. This way the intensity of KU2 spectra that have four equivalent positions becomes twice higher than that of KU3 arising from two equivalent positions. In general, the oxygen atom captured at one of these four bonds leads to the triclinic symmetry of the center but the experimental angular dependence of KU2 in Fig. 6 shows the monoclinic symmetry of the ***g***- and ***D***-tensors. This suggests that the shift of the Si atom at b in (001) plane takes into account the large angle 110° between the b-e and b-f bonds. Also the resolution of EPR spectrometer, ~0.1 mT, may not be sufficient to detect the additional splittings of KU2 EPR lines. As follows from the above models, the distance r_{ab} between Si atoms at a and b must be smaller compared with that of the undistorted A-center and increases the components of ***D***-tensors which are proportional to $1/r_{ab}^3$ for KU2 and KU3. The estimated distance r_{ab} is about 3.72 Å for KU2 and 3.63 Å for KU3, and they are smaller than 3.83 Å of undistorted SL1.

IV. CONCLUSIONS

In conclusion, two new spin $S = 1$ EPR spectra labeled KU2 and KU3 were observed in γ-irradiated Czochralski grown silicon crystals after annealing in the temperature range 360–560 °C. These spectra emerged when the EPR intensity of SL1, the excited triplet state of A-center, decreased. Analysis of the fine and hyperfine structures of both KU2 and KU3 spectra allowed us to conclude that they arose most likely from the excited triplet states of the A center when an extra oxygen atom was captured by the Si bonds near the A-center to induce lattice distortion. Microscopic models for KU2 and KU3 centers were suggested.

ACKNOWLEDGMENTS

The work at Keio University was supported in parts by the Grant-in-Aid for Scientific Research by MEXT, NanoQuine, JSPS Core-to-Core Program, and Cooperative Research Project Program of the RIEC, Tohoku University. This work at St. Petersburg was supported by the grant of the Government of Russia, Project 14.Z50.31.0021.

[1]J. Troxell, Solid-State Electron. **26**, 539 (1983).
[2]C. A. J. Ammerlaan, "Paramagnetic centers in silicon," in *Landolt-Börnstein Numerical Data and Functional Relationship in Science and Technology*, Impurity and Defects in Group IV Elements and III-V Compounds Vol. 22, edited by O. Madelung (Springer-Verlag, Berlin, 1992), p. 365.
[3]G. D. Watkins, "A review of EPR studies in irradiated silicon," in *Radiation Damage in Semiconductors*, edited by P. Baruch (Dunod, Paris, 1965), p. 97.
[4]G. Bemski, J. Appl. Phys. **30**, 1195 (1959).
[5]G. D. Watkins, J. W. Corbett, and R. M. Walker, J. Appl. Phys. **30**, 1198 (1959).
[6]K. L. Brower, Phys. Rev. B **4**, 1968 (1971).
[7]W. Akhtar, T. Sekiguchi, T. Itahashi, V. Filidou, J. J. L. Morton, L. Vlasenko, and K. M. Itoh, Phys. Rev. B **86**, 115206 (2012).
[8]J. W. Corbett, G. D. Watkins, and R. S. McDonald, Phys. Rev. **135**, A1381 (1964).
[9]Y.-H. Lee and J. W. Corbett, Phys. Rev. B **13**, 2653 (1976).
[10]A. Chroneos, E. N. Sgourou, C. A. Londos, and U. Schwingenschlögl, Appl. Phys. Rev. **2**, 021306 (2015).
[11]N. Yarykin and J. Weber, Physica B **401–402**, 483 (2007).
[12]N. Yarykin and J. Weber, Physica B **404**, 4576 (2009).
[13]M. Otsuka, T. Matsuoka, L. S. Vlasenko, M. P. Vlasenko, and K. M. Itoh, Appl. Phys. Lett. **103**, 111601 (2013).